Computer Simulations of Ionomer Self-Assembly and Dynamics

Monojoy Goswami,[†] Sanat K. Kumar,*[,†] Aniket Bhattacharya,[‡] and Jack F. Douglas[§]

Department of Chemical Engineering, Columbia University, New York, New York 10027; Department of Physics, University of Central Florida, Orlando, Florida 32816; and Polymers Division, National Institutes of Standards and Technology, Gaithersburg, Maryland 20899

Received January 10, 2007

Revised Manuscript Received April 30, 2007

Introduction. When charged polymers are present in dilute solution in a polar solvent, the counterions are typically released into solution due to the dominance of entropic effects ("polyelectrolyte" behavior). In the opposite case of a medium with very low dielectric constant ("ionomer" melt state), the energetic cost associated with counterion release dominates, and hence the neutralizing counterions are closely coupled to the chains in the form of transient local dipoles.[1−7] It has been speculated that these dipoles stick together into small multiplets, which serve to bridge chains and create a long-lived transient polymer network.[8−11] This network formation is consistent with the unusual transport behavior of ionomers.[12,13] The spatial coupling of the counterions with the chains and the resulting interesting transport properties have made ionomers relevant to a range of applications, e.g., in coatings,[14,15] proton exchange membranes,[16−18] biomedical implants,[19,20] and binders in composites.[21,22]

To understand the morphological and dynamical properties of ionomer melts requires an explicit treatment of Coulomb interactions. While previous workers, primarily the group of Khokhlov,[23−28] have theoretically sought to understand the relationship between transient dipoles and network formation, most simulation studies have ignored Coloumb effects[29−31] because of the difficulty in accounting for these long-range interactions. To elaborate: the long-ranged Coloumb interaction varies with distance, r, as $1/r$. Thus, the calculations of thermodynamic quantities, such as the system energy, which require a spatial integration of this potential do not readily yield a converged value. (Standard tricks that work for short-ranged potentials, such as cutting off the potential at some (short) distance r_c and including the contribution from all larger distances by assuming the pair distribution, $g(r) = 1$, will thus not be appropriate.) While there is a suite of simulation tools (e.g., Ewald sums) that have been developed to circumvent these difficulties and give finite converged values for thermodynamic quantities, the point being made is that these are computationally expensive (and often intractable). In contrast to these practical matters, it seems evident that including Coloumb interactions will be crucial for determining the temperature at which the ions pair into dipoles and presumably the self-assembly of ionomers into transient networks. Further, the inclusion of explicit counterions is necessary to properly understand the mechanisms of charge transport in such materials. Recent molecular dynamics (MD) simulations which explore charge transport in ionomer solutions do account explicitly for ionic interactions.[23,26,32−36] While these last class of simulations have focused on the relevant problem of charge transport and on the relationship between morphology and transport, little attention has been paid to the self-assembly phenomenon which apparently is critical to the behavior of ionomers. To our knowledge, most work focused on the self-assembly of ionomers have modeled the behavior of solutions of chains where ionic interactions have been simplified, and each transient dipole (i.e., a transient ion−counterion pair) is replaced by a "sticker".[37−41]

To make progress in this area, we start with the polymer analogue of the "primitive model" of electrolyte solutions[42−44] where each chain is modeled as a string of catenated hard spheres. We have performed molecular dynamics simulations on melts of telechelic chains where each chain end has a charge of $-q$. An equal number of hard-sphere counterions (with the same size as the chain monomers) are introduced to maintain charge neutrality. This is a basic reference model from a computational standpoint, and we explore the extent to which this minimal model of ionomers can reproduce experimental trends, e.g., the tendency to form multiplet structures having the form of sheetlike or compact globular forms, the presence of multiple glass transitions governing properties, and evidence for transitions in the counterion mobility.

Simulation Methods. We use the bead−spring polymer model[45] and augment this with Coulomb interactions. The interaction between any pair of beads is modeled by a soft repulsive potential:

$$U_{ij}^{\mathrm{LJ}} = 4\epsilon_{\mathrm{LJ}}\left[\left(\frac{\sigma}{r_{ij}}\right)^{12} - \left(\frac{\sigma}{r_{ij}}\right)^{6} + \frac{1}{4}\right] \tag{1}$$

for distances $r_{ij} \leq 2^{1/6}\sigma$, beyond which it is set to zero. Bonded beads are connected by FENE springs:[45]

$$U_{ij}^{\mathrm{chain}}(r_{ij}) = -\frac{1}{2}kR_{ij}^{\ 2}\ln\left[1 - \left(\frac{r_{ij}}{R_{ij}}\right)^{2}\right] \tag{2}$$

where $k = 37.5(\epsilon_{\mathrm{LJ}}\sigma^2)$ and $R_{ij} = 1.5\sigma$ is the maximum bond length. Both the bead diameter and the equilibrium bond length are on the order of σ. We consider "telechelic" chains where each chain end has a charge of $-q$. To maintain charge neutrality, we include small molecule counterions of the same size and nonpolar interactions as a chain monomer, but with a charge of $+q$. (Note that the counterions are not chemically bonded to the chains.) While we have examined a variety of N values, here we focus on the single case of $N = 64$. In a related set of calculations, we have considered chains of length $N = 66$. However, the last two monomers at each end of the chains were respectively a $+q$ and $-q$. This system, in effect, places a dipole at each end of a chain, a model which has been used to describe the behavior of ionomers.[4,6,7,37] Our calculations on this "dipole" model, when compared to nonbonded counterions, allows us to critically delineate the importance of the counterion entropy. The charges interact via the Coulomb potential

$$U_{ij}^{\mathrm{C}} = \frac{q_i q_j}{\epsilon_{\mathrm{r}} r_{ij}} \tag{3}$$

where ϵ_{r} is the dielectric constant of the medium (which is order 1 in ionomers and $\gg 1$ for polyelectrolytes). Long-range Coulomb interactions are accounted for through an Ewald sum.[46]

[†] Rensselaer Polytechnic Institute.
[‡] University of Central Florida.
[§] National Institutes of Standards and Technology.

10.1021/ma070074w CCC: $37.00
Published on Web 05/17/2007

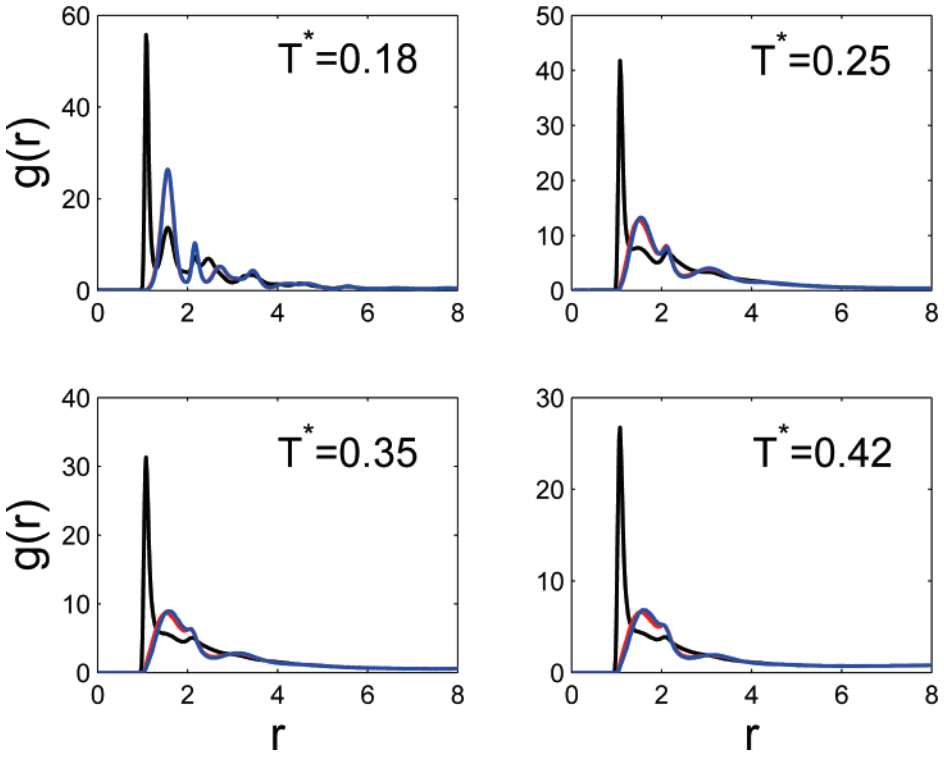

Figure 1. Counterion−counterion (blue lines), end-group ion−end-group ion (red), and end-group ion−any charge (black) $g(r)$ at four different temperatures.

The reduced temperature is $T^* = k_B T/\epsilon_{LJ}$. A second energy scale is the ratio of Coulomb and Lennard-Jones interactions:

$$\epsilon_B = \frac{q^2}{\epsilon_r \sigma \epsilon_{LJ}} \tag{4}$$

For real experimental systems, ϵ_B ranges between 10 and 100: we use $\epsilon_B = 10$. While we shall use the conventional definition of the reduced temperature, another definition that is more relevant to the polyelectrolyte/ionomer community is $T^*_{elec} = \epsilon_r \sigma k_B T/q^2 \equiv T^*/\epsilon_B$. All quantities are reported in reduced units.[47] We consider melts with monomer number density $\rho^* = \rho\sigma^3 = 0.69$ (ρ is the monomer number density). This value is in the range of typical values (0.6−0.85) used to describe polymer melts. Langevin molecular dynamics simulations[48] are carried out in a cubic box of length 16 with periodic boundary conditions with 43 chains and 86 counterions. A few calculations used boxes with a lateral size ≈20 (90 chains and 180 counterions). The governing MD equations are

$$m_i \frac{d\vec{v}_i}{dt} = -\nabla \vec{U}_i - \Gamma \frac{d\vec{r}_i}{dt} + \vec{W}_i(t) \tag{5}$$

where U_i is the potential energy experienced by particle i and m_i is its mass. Γ is the friction coefficient, and $\vec{W}_i(t)$ is a Gaussian random force with zero mean, where $\langle \vec{W}_i(t) \cdot \vec{W}_j(t') \rangle = 6 m_i k_B T \Gamma \delta_{ij} \delta(t - t')$. Thus, we simulate in the canonical ensemble. After equilibration (2 to 10×10^7 steps), we run for at least 2×10^8 steps: an MD time step corresponds to $t^* \equiv t/\sqrt{m\sigma^2/\epsilon_{LJ}} = 0.01$.

Results and Discussion. We primarily focus on the case with nonbonded counterions, and augment this discussion as necessary with the dipolar system, in which each ion is chemically paired to a counterion. (If the system is not described, then we are dealing with the situation of unbonded counterions.) The radial distribution functions, $g(r)$, for the three different types of ion pairs are plotted in Figure 1. The $g(r)$ show increasing structure (also see Figure 3) with decreasing T^*, particularly below $T^* = 0.25$, suggesting that there is an effective attraction between like charge ions which causes structure formation at low T^*. In particular, we note the presence of up to four peaks in the like ion pair distribution function at $T^* = 0.18$. We deduce that these materials undergo self-assembly between $T^* = 0.25$ and 0.18.

To understand the role of counterions on this structure formation, we consider two definitions of the fraction of free counterions. The first one locates counterions that have no other charge within the first like-ion pair correlation peak ($r \leq 1.96$). The second asks if a counterion has any other counterion neighbor within the same distance. Thus, while the first definition is sensitive to the presence of isolated charges, the second focuses on the existence of dipoles and their state of pairing. From Figure 2a it is apparent that there is a very small fraction of isolated counterions over the whole range of T^* considered. However, since the fraction of free dipoles is ≈0.1 for $T^* \geq 0.25$, charge pairing is strongly preferred over this temperature range. This conclusion is bolstered by the fraction of isolated dipoles in the dipolar system: it is seen that these results closely track the case of free counterions. We thus conclude that the pairing of charges of opposite sign occurs at temperatures well above $T^* = 0.4$. Further, the fraction of free "dipoles" decreases dramatically in the vicinity of $T^* = 0.21$, which is in the temperature range where we presume that the system undergoes ordering.

Parts b and c of Figure 2 show the heat capacity (C_v) and the structural relaxation time (τ^*) as a function of inverse temperature (see below for definitions). We see a relatively abrupt change in behavior in both the properties for $T^* \approx 0.21$. C_v was calculated following the fluctuation formula

$$C_v \propto \frac{\langle U^2 \rangle - \langle U \rangle^2}{T^2} \tag{6}$$

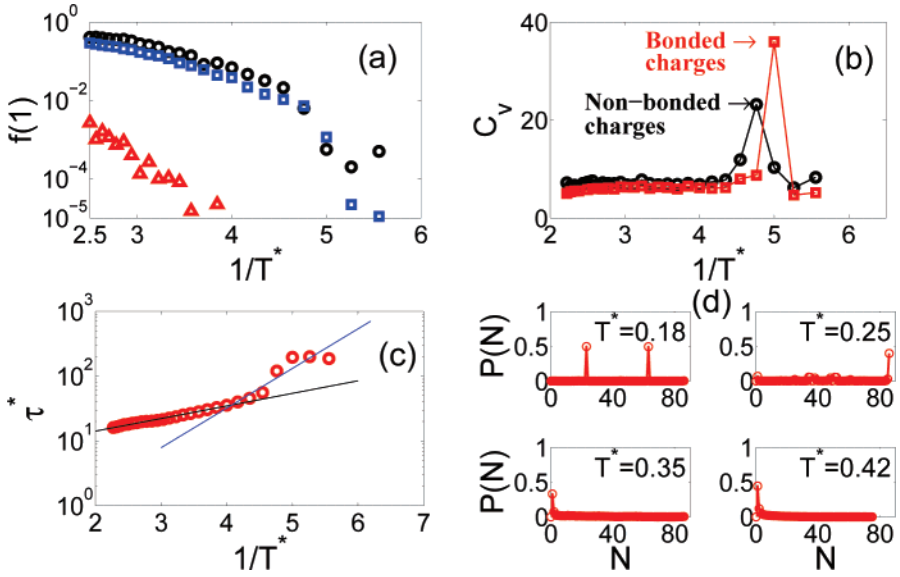

Figure 2. (a) Fraction of free counterions vs $1/T^*$. The triangles are isolated counterions, and the black circles are counterions with no near counterion. The blue squares are the fraction of free dipoles from the dipolar case. (b) C_v as a function of $1/T^*$. (c) Structural relaxation times obtained from the self-intermediate scattering function of the counterions as a function of $1/T^*$. The lines are fits to guide the eye. (d) Cluster size distribution at different temperatures.

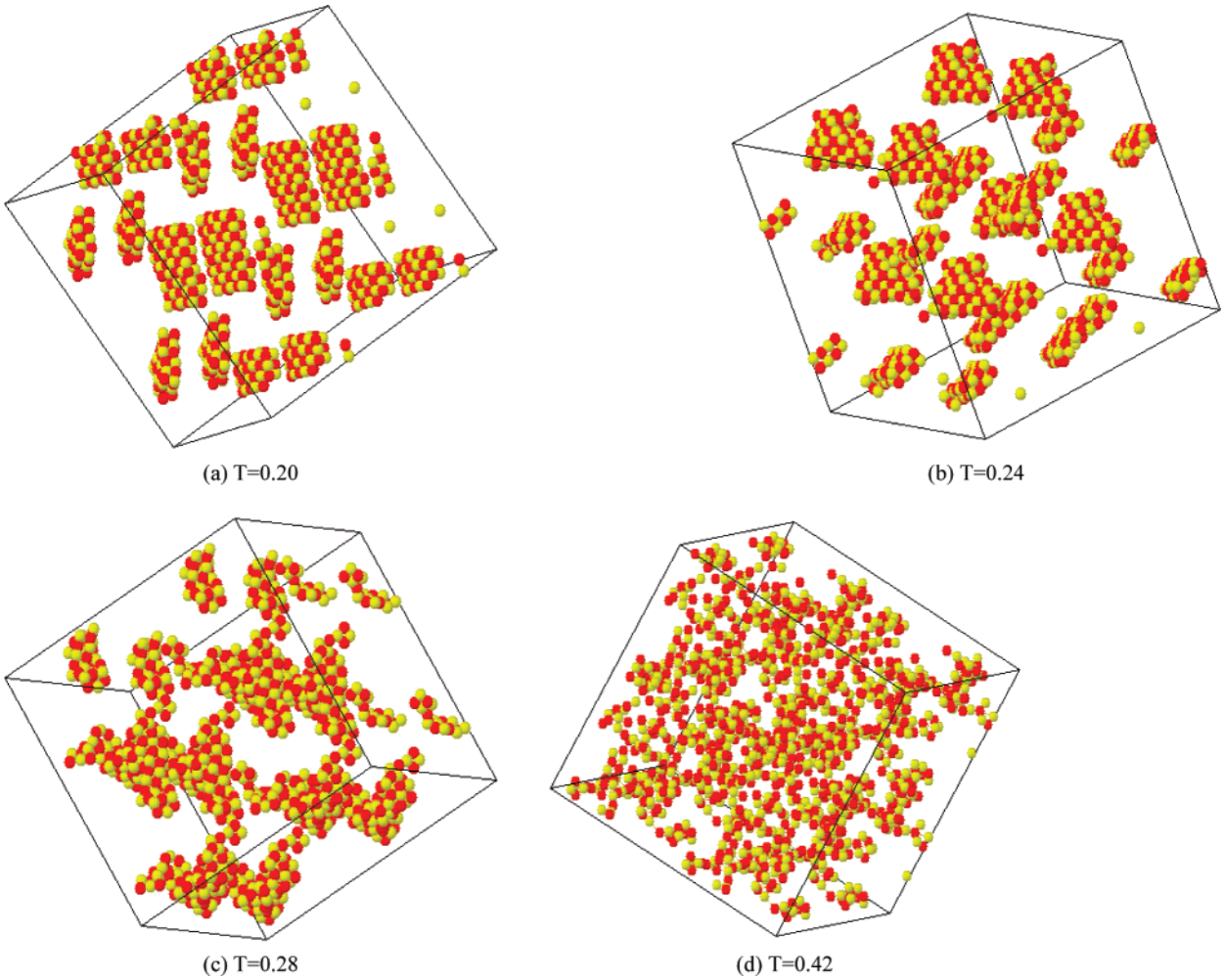

Figure 3. Snapshots at (a) $T^* = 0.20$, (b) $T^* = 0.24$, (c) $T^* = 0.28$, and (d) $T^* = 0.42$. For clarity purposes only the charges are shown in the snapshots. Red dots are chain-end charges, and yellow dots are counterions. The snapshots correspond to the main periodic cell and eight of its nearest image cells. Note that an apparently percolated structure begins to break down in the vicinity of $T^* = 0.24$.

where U is the potential energy and $\langle ... \rangle$ denotes an ensemble average. The appearance of a peak in the C_v data indicates the temperature where the ionomers undergo self-assembly. Empirically, this type of feature is often referred to as a "glass transition" in the ionomer field.[49,10] We do not see a second "T_g" process: we suggest that this is because these chains (in

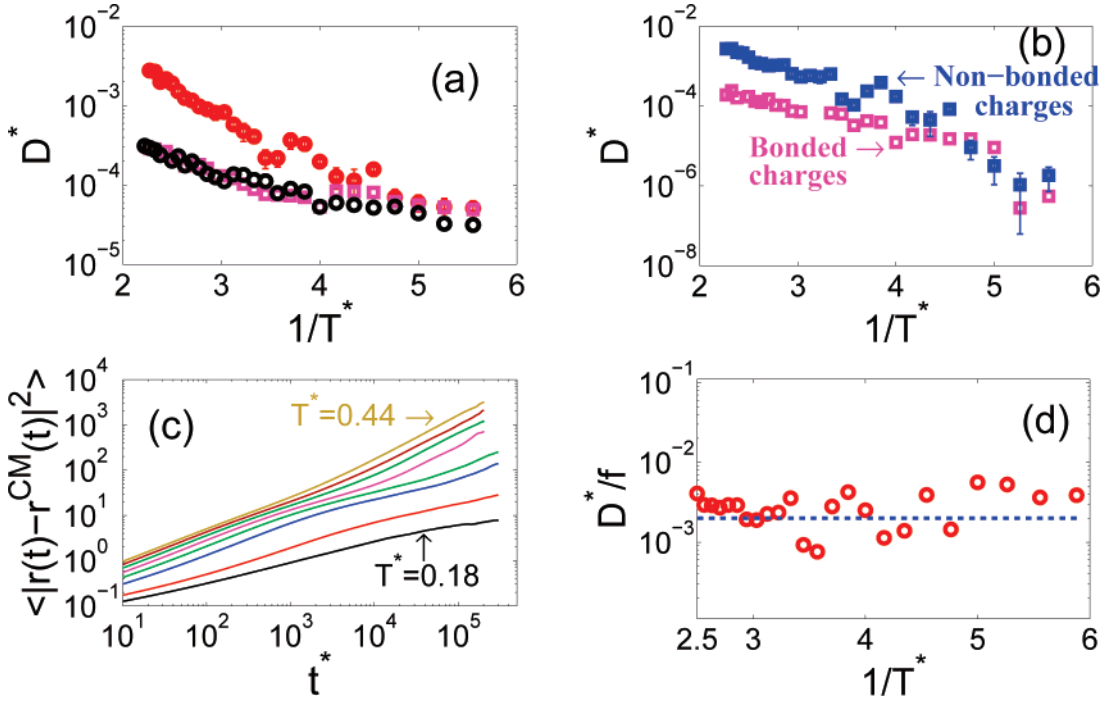

Figure 4. (a) Counterion diffusion (red circles) and chain center-of-mass diffusion (open squares). The diffusion of counterions in the case of dipolar fluid are also shown (black circles). (b) Counterion diffusion coefficient obtained after subtracting the center-of-mass motion of all the counterions. (c) Mean-square-displacement after subtracting the center-of-mass of the counterions. From bottom to top the T^* goes as 0.18, 0.21, 0.24, 0.28, 0.32, 0.36, 0.40, and 0.44. (d) Temperature dependence of ratio of finite size corrected diffusion coefficients and fraction of free dipoles for the case of nonbonded counterions.

the absence of charges) do not vitrify at this density. Since the C_v peak occurs regardless of whether the ions are chemically bonded or not, it is evidently related to the clustering of dipoles and associated multiplet formation. The structural relaxation time was obtained from plots of the self-intermediate scattering function, $F_s(q^*,t^*)$, for q^* values corresponding to the first peak value of the structure factor, $S(q^*)$, of the counterions. The structural relaxation time corresponds to the time, t, where $F_s(q^*,t^*)$ assumes a value of $1/e$. In combination, these results support the notion that these ionomers undergo a structural transition, akin to the microphase separation in block copolymers, in the vicinity of $T^* \approx 0.22$. Below this temperature, the relaxation times of the material increase strongly, consistent with the strong localization of charged moieties into multiplet clusters.

Figure 2d shows the cluster size distributions for systems with free counterions over a range of temperatures. To define a cluster, we only consider charges of the same kind (i.e., counterions) that are separated by $r \leq 1.96$. System snapshots (Figure 3) allow for clarification. At the lowest temperature ($T^* \leq 0.21$) we see that there are two nonpercolating clusters and hardly any free dipoles. We are unable to get reliable results for $T^* \leq 0.18$ where, as we shall show below, the system does not equilibrate in our relatively long simulations. For $T^* \leq 0.21$ the system forms ribbonlike structures (see Figure 3) with an antiparallel ordering of dipoles. While these sheets have thicknesses comparable to the size of a dipole, the factors that control their lateral dimensions have not been explored. Note also that there is no higher order arrangement of these sheets, probably due to the conformational entropy of the (flexible) chain backbone which prevents such ordering. This behavior is in contrast to bola-amphiphiles, where sheets of charges can arrange into smectic phases. This occurs either because the backbone is short and stiff or because such assembly is favored due to hydrogen-bonding interactions between the backbones. At higher temperatures ($T^* > 0.25$), these systems form less well ordered, but percolating, structures. These percolating structures disappear at even higher temperatures ($T^* > 0.35$). These results are in agreement with previous models of ionomer organization[38,49−51] and also with experimental observations.[52−54] We see that the self-assembly of ionomer melts exhibits features in common with both block copolymers (where organization is dominated by packing effects) and directional self-assembly (where the core structures develop sheets that are consistent with the symmetry characteristics of the quadrupole potential).[55] Ionomer self-assembly is thus a hybrid between these two classes of assembly mechanisms.

To understand the consequence of this self-assembly process on transport properties, we have calculated the diffusion coefficients of the counterions and the centers of mass of the chains at different temperatures. As the melt system under investigation is homogeneous and isotropic, the diffusion coefficient is treated as a scalar quantity. We used the Einstein relationship $\langle r^2 \rangle = 6Dt$ to estimate these diffusion constants, where $\langle r^2 \rangle$ is the mean-squared displacement of the appropriate species (see Figure 4a). At high temperatures (above $T^* \geq 0.25$) it is apparent that the counterions are significantly more mobile than the chains. However, the diffusion of counterions chemically bound to the chain ("dipolar" case) tracks that of the center of mass, as expected. In this range of temperatures, the diffusion constants appear to have an Arrhenius temperature dependence. For $T^* \leq 0.22$, however, the slope of the diffusion coefficient vs $1/T^*$ decreases. We shall show below that this change in slope is a purely finite size effect in the simulations. To clarify this point, we have calculated the center of mass of the 86 (or 180 for the larger system) counterions in the system and find that this quantity "drifts" as a function of time, even though the system as a whole has zero momentum. For such small systems we only see two clusters when we deal with 43 chains. This increases to four for the larger system. Thus, even though these clusters drift at "random", the sum of their drift velocities is not necessarily zero. We argue that, in this strong segregation limit, this small finite size effect is much larger than the actual

diffusion of charges (in fact dipoles). Evidence supporting this finite-size drift mechanism is that the mean-squared motion of the center of mass of all the counterions decreases linearly with system size. Since this "drift" phenomenon may thus be expected to disappear in the truly thermodynamic limit, the diffusion constant derived from counterion motion relative to the center of mass of the charges represents the true transport behavior of the counterions. We thus calculated the $\langle r^2 \rangle$ of the counterions relative to the center of mass; i.e., we calculated $\langle [\{r_i(t) - r_{CM}(t)\} - \{r_i(0) - r_{CM}(0)\}]^2 \rangle$. A new diffusion constant, which is representative of counterion motion *relative* to the center of mass of the ion cluster (and presumably corrected for this finite size drift), was then obtained.

As a consequence of this subtraction, the diffusion of nonbonded counterions follows a single Arrhenius temperature dependence over the whole temperature range considered (Figure 4b). The activation energy obtained from this plot is $\approx$1.5, which is comparable to the ion pairing energy at contact. This subtraction procedure has the highest impact at the lowest temperatures ($T^* \leq 0.22$) where the dipoles exhibit the strongest clustering. It is also apparent from Figure 4b that the nonbonded and dipolar systems behave identically in this low-temperature range where the charges form ribbonlike structures in both cases. Since the charges are strongly spatially localized at the lowest temperatures, it is hard to pull one out from a cluster to effect diffusion.

At higher temperatures it is clear that the nonbonded counterions move faster than in the "dipolar" fluid. Thus, we see that, even though the charges are strongly paired into dipoles, the transport is still dominated by unpaired ions. This changes dramatically when the dipoles pair into clusters. A more careful examination of this diffusion constant, especially for temperatures lower than $T^* = 0.22$, suggests that $D \approx 10^{-6}$. Since our longest simulation times are $t^* \approx 2 \times 10^6$, it then follows that the $\langle r^2 \rangle$ of the counterions relative to the center of mass is $6Dt^* \approx 12$. Since the mean-squared radius of gyration of the chains is $\approx$12, it is thus readily apparent that, for lower temperatures, the counterion motion relative to the center of mass is so sluggish that the equilibration of these systems is not guaranteed in our relatively long simulations. We also plot the mean-squared displacement of counterions relative to the center of mass in Figure 4c to illustrate this point: these results suggest that temperatures as low as $T^* = 0.18$ might still be at equilibrium. Lower T^* are probably not equilibrated.

Clearly, the dynamics accompanying ionomer self-assembly has features in common with gels and glasses, with the formation of charged multiplets being the localization mechanism. Evidence substantiating this suggestion is presented in Figure 4d where we plot the ratio of the counterion diffusion constant (nonbonded ions, relative to the center of mass) and the fraction of free dipoles as a function of temperature. At low temperatures it is apparent that, within the relative large uncertainties, this quantity is independent of temperature. Thus, the transport behavior of these systems are crucially dependent on unpaired dipoles, even though the counterions are not bonded chemically to the chain. Since this fraction of free dipoles drops below $T^* \approx 0.21$, the counterion mobilities drop precipitously as well. This is consistent with previous simulations of self-assembly in uncharged telechelic polymers.[37]

Relationship of This Work to Other Simulation and Experimental Work. Our model is closest in spirit to the restricted primitive model (RPM),[42−44] which corresponds to a fluid comprised of hard spheres with half possessing a single positive charge while the other half has a single negative charge (i.e., no chains are present). This model system has been been well studied, and it is well accepted that it phase separates below $T^*_{elec} \approx 0.05$. Our simulations show no signature of phase separation in the chain analogue, but rather clear indications of a microphase separation transition at $T^*_{elec} = 0.021$. It is physically reasonable that the microphase separation transition occurs at temperatures that are considerably lower than the RPM critical temperature for phase separation, but we are unable to provide any quantitative insights into this difference. We now attempt to make contact between this estimate of a microphase separation transition and experiment. For a typical ionomer $\epsilon_r = 2.5$, while $\sigma \approx 3.5$ Å. Using these values in the definition of T^*_{elec} allows us to estimate that the microphase separation transition occurs at $T \simeq 415$ K (142 °C), which is the right range of temperatures where Eisenberg[49] found a second glass transition for several ionomers. We thus classify this experimental "glass transition" as being the self-assembly transition. While more accurate models have to be used to solidify this conclusion, it definitely stresses that the simplest "primitive" model for an ionomer yields the correct qualitative behavior.

Conclusions. Our major finding is that ionomers self-assemble through a process where there is formation of ionic multiplets. This self-assembly has the distinct signatures of "vitrification", i.e., a peak in the specific heat and spatial localization of ions, which have lead previous investigators to discuss this transition as a second "glass" transition in these materials.[10] This type of assembly has features in common with the self-assembly of block copolymer systems, where there is also an organization of structures at equilibrium with well-defined characteristic dimensions, but there are also features that arise in these systems that are found in systems with strong directional interactions. We also establish by simulating with the counterions paired and unpaired that the intuition that dipolar interactions dominate the multipole assembly is well founded. However, this viewpoint does not accurately extend to understanding the transitions in the counterion mobility where the unbinding transition between the ions and counterions plays a central role.

Now that we have established that the computational model is sufficient to recover basic qualitative aspects of self-assembly in real ionomer fluids, we are in a position to investigate the effect of some of the variables that are expected to be relevant for these systems. Initial studies will focus on the influence of ion size and valence asymmetry in the self-assembly, morphology, and dynamics. We shall also study the effect of varying the chain length, the position of the ionic species, random and regular ion spacings within the chains, the effect of the dielectric constant, and the spatial dependence of the dielectric constant. We expect the addition of polarizability effects to both the ions and the neutral species to be very relevant for understanding the properties of real ionomer fluids. The present work is just a first step to understanding the properties of these fluids which combines information from experiment, simulation, and analytic theory.

Acknowledgment. The authors thank the Department of Energy (DE-FG02-05ER46258) for financial support of this work.

References and Notes

(1) Eisenberg, A.; Kim, J. *Introduction to Ionomers*; John Wiley & Sons: New York, 1998.
(2) Schlick, S. *Ionomers: Characterization, Theory, and Application*; CRC Press: Boca Raton, FL, 1996.
(3) Mauritz, K.; Moore, R. B. *Chem. Rev.* **2004**, *104*, 4535−4585.

(4) Tant, M. R.; Mauritz, K. A.; Wilkes, G. L. *Ionomers Synthesis, Structure, Properties and Applications*; Blackie Academic and Professional: London, 1997.
(5) Page, K. A.; Cable, K. M.; Moore, R. B. *Macromolecules* **2005**, *38*, 6472.
(6) Capek, I. *Adv. Colloid Interface Sci.* **2005**, *118*, 73.
(7) Semenov, A. N.; Nyrkova, I. A.; Khokhlov, A. R. *Macromolecules* **1995**, *28*, 7491.
(8) Leibler, L.; Rubinstein, M.; Colby, R. H. *Macromolecules* **1991**, *24*, 4701.
(9) Tanaka, F.; Edwards, S. F. *Macromolecules* **1992**, *2*, 1516.
(10) Eisenberg, A.; Bird, B.; Moore, R. B. *Macromolecules* **1990**, *23*, 4098.
(11) Kumar, S. K.; Douglas, J. F. *Phys. Rev. Lett.* **2001**, *87*, 188301.
(12) Colby, R. H.; Zheng, X.; Rafailovich, M. H.; Sokolov, J.; Peiffer, D. G.; Schwarz, S. A.; Strzhemechny, Y.; Nguyen, D. *Phys. Rev. Lett.* **1998**, *24*, 4701.
(13) Kutsumizu, S.; Schlick, S. *J. Mol. Struct.* **2005**, *739*, 191.
(14) Whiteley, L. D.; Martin, C. R. *Anal. Chem.* **1987**, *59*, 1746.
(15) Matysik, F.-M.; Matysik, S.; Brett, A. M. O.; Brett, C. M. A. *Anal. Chem.* **1997**, *69*, 1651.
(16) Jiang, S.; Xia, K.-Q.; Xu, G. *Macromolecules* **2001**, *34*, 7783.
(17) Rubatat, L.; Rollet, A. L.; Gebel, G.; Diat, O. *Macromolecules* **2002**, *35*, 4050.
(18) Rubinstein, I.; Bard, A. J. *J. Am. Chem. Soc.* **1981**, *103*, 5007.
(19) Amitay-Sadovsky, E.; Komvopoulos, K.; Ward, R.; Somorjai, G. A. *J. Phys. Chem. B* **2003**, *107*, 6377.
(20) Berrocal, M. J.; Badr, I. H. A.; Gao, D.; Bachas, L. G. *Anal. Chem.* **2001**, *73*, 5328.
(21) Lewis, J. P.; Sewell, T. D.; Evans, R. B.; Voth, G. A. *J. Phys. Chem. B* **2000**, *104*, 1009.
(22) Smith, G. D.; Bedrov, D.; Byutner, O.; Borodin, O.; Ayyagari, C.; Sewell, T. D. *J. Phys. Chem. A* **2003**, *107*, 7552.
(23) Hu, N.; Chen, R.; Hsu, A. *Polym. Int.* **2006**, *55*, 872.
(24) Jang, S. S.; Molinero, V.; Cagin, T.; Goddard, W. A., III *J. Phys. Chem. B* **2003**, *108*, 3149.
(25) Blake, N. P.; Peterson, M. K.; Voth, G. A.; Metiu, H. *J. Phys. Chem. B* **2005**, *109*, 24244.
(26) Vishnyakov, A.; Neimark, A. V. *J. Phys. Chem. B* **2001**, *105*, 9586.
(27) Khalatur, P. G.; Khokhlov, A. R.; Nyrkova, I. A.; Semenov, A. N. *Macromol. Theory Simul.* **1996**, *5*, 713.
(28) Wang, Z.; Rubinstein, M. *Macromolecules* **2006**, *39*, 5897.
(29) Banaszak, M.; Clarke, J. H. R. *Phys. Rev. E* **1999**, *60*, 5753.
(30) Wong, C.; Clarke, J. H. R. *J. Chem. Phys.* **2002**, *116*, 6795.
(31) Sung, B. J.; Yethiraj, A. *J. Chem. Phys.* **2003**, *119*, 6916.
(32) Choi, P.; Jalani, N. H.; Dutta, R. *J. Electrochem. Soc.* **2005**, *152*, E123−E130.
(33) Jinnouchi, R.; Okazaki, K. *J. Electrochem. Soc.* **2003**, *150*, E66.
(34) Paddison, S. J. *Annu. Rev. Mater. Res.* **2003**, *33*, 289.
(35) Polizos, G.; Shilov, V. V.; Pissis, P. *J. Non-Cryst. Solids* **2002**, *305*, 212.
(36) Spohr, E.; Commer, P.; Kornyshev, A. A. *J. Phys. Chem. B* **2002**, *106*, 10560.
(37) Bedrov, D.; Smith, G. D.; Douglas, J. F. *Europhys. Lett.* **2002**, *59*, 384.
(38) Khalatur, P. G.; Khokhlov, A. R.; Mologin, D. A. *J. Chem. Phys.* **1998**, *109*, 9614.
(39) Khalatur, P. G.; Khokhlov, A. R.; Kovalenko, J. N.; Mologin, D. A. *J. Chem. Phys.* **1999**, *110*, 6039.
(40) Kim, S. H.; Jo, W. H. *Macromolecules* **2001**, *34*, 7210.
(41) Timoshenko, E. G.; Kuznetsov, Y. A. *Europhys. Lett.* **2001**, *53*, 322.
(42) Panagiotopoulos, A. Z. *Fluid Phase Equilib.* **1992**, *76*, 97.
(43) Fisher, M. E.; Levin, Y. *Phys. Rev. Lett.* **1993**, *71*, 3826.
(44) Caillol, J. M. *J. Chem. Phys.. 102*, 100.
(45) Grest, G. S.; Kremer, K. *Phys. Rev. A* **1986**, *33*, 3628.
(46) Leeuw, S. W. D. *Proc. R. Soc. London A* **1980**, *373*, 27.
(47) Allen, M. P.; Tildesley, D. J. *Computer Simulation of Liquids* (reprint ed.); Oxford University Press: New York, 1989.
(48) van Gunsteren, W. F.; Berendsen, H. J. C. *Mol. Phys.* **1982**, *45*, 637.
(49) Eisenberg, A. *Macromolecules* **1970**, *3*, 147.
(50) Khalatur, P. G.; Khokhlov, A. R.; Mologin, D. A. *J. Chem. Phys.* **1998**, *109*, 9602.
(51) Semenov, A. N.; Joanny, J.-F.; Khokhlov, A. R. *Macromolecules* **1995**, *28*, 1066.
(52) Winey, K. I.; Laurel, J. H.; Kirkmeyer, B. *Macromolecules* **2000**, *33*, 507.
(53) Kirkmeyer, B.; Weiss, R.; Winey, K. I. *J. Polym. Sci., Part B: Polym. Phys.* **2001**, *39*, 477.
(54) Kirkmeyer, B.; Taubert, A.; Kim, J.-S.; Winey, K. I. *Macromolecules* **2002**, *35*, 2648.
(55) Workum, K. V.; Douglas, J. F. *Phys. Rev. E* **2006**, *73*, 031502.

MA070074W